COBEM 99
XV Congresso Brasileiro de Engenharia Mecânica
15th Brazilian Congress of Mechanical Engineering
22 - 26 de Novembro de 1999 / November 22 - 26, 1999 Águas de Lindóia, São Paulo,

DYNAMIC RESPONSE OF AXISYMMETRIC ELASTIC BODIES BY THE BOUNDARY ELEMENT METHOD

Ronaldo Carrion
Euclides de Mesquita Neto
Departamento de Mecânica Computacional, Faculdade de Engenharia Mecânica,
Universidade Estadual de Campinas - UNICAMP, C.P. 6122, CEP 13083-970 Campinas, SP
Sérgio Santos Mühlen
Departamento de Engenharia Biomédica, Faculdade de Engenharia Elétrica e de Computação,
Universidade Estadual de Campinas - UNICAMP, C.P. 6040, CEP 13083-970 Campinas, SP

Abstract. *A Boundary Element formulation to analyze the dynamic response of elastic axisymmetric bodies is presented. In the formulation the 3D kernels were transformed into axisymmetric kernels by a coordinate change and an integration over the azimuthal direction. The dynamic singular kernels are regularized subtracting the corresponding static kernels. The static singular kernels are solved by the rigid body argument. The BE implementation is validated by determining the response of a cylinder with known modal data, i.e. eigenfrequencies and eigenmodes. The methodology is also applied to analyze the response of an acoustic horn.*

Key words: *Boundary Element Methods, Axisymmetric bodies, Vibration.*

1. INTRODUCTION

In the present article the dynamic response of axisymmetric linear elastic bodies is analyzed using an implementation of the Boundary Element Method (BEM). The main advantage of the BEM over the Domain Methods (Finite Difference and Finite Element Methods) is the reduction by one in the order of the discretization process. In the 3D BEM formulation of non-axisymmetric problems it is necessary to discretize the domain surface [Kane, 1994; Dominguez, 1993]. In the case of axisymmetric bodies only the line generating the revolution surface needs to be discretized, leading to a great reduction in pre-processing time [Becker, 1992].

The axisymmetric implementation of the BEM is accomplished integrating the kernels of the dynamic 3D fundamental solutions [Dominguez, 1993] once over the azimuthal angle and in the sequence over the line generating the revolution surface. The displacement and traction kernels of the 3D fundamental solutions present, respectively, a weak (integrable) singularity and a strong singularity, which must be integrated in the Cauchy Principal Value (CPV) sense. In the present formulation the weak singular kernels are transformed into an equivalent elliptic

integrals, and evaluated numerically. The strong singular integrals are regularized by means of the static 3D traction kernels. The corresponding axisymmetric static problem is solved using a rigid body argument as well as a particular solution for stresses [Becker, 1992; Carrion, 1999].

There is good physical and numerical motivation for an Axisymmetric BEM implementation. Vibrating axisymmetric bodies are being widely used in ultrasonic wave generating devices. The typical device can be pictured in Figure 1. It consists of an active piezoelectric ceramic element connected to a passive axisymmetric elastic concentrator. The role of the concentrator is to amplify the vibration amplitude induced by the piezoelectric ceramic, generating thus an ultrasonic field at the free extremity. The ultrasonic transducers are acoustically very inefficient. One of the reasons lies in the fact that not only the free extremity generates an acoustic field, but the whole vibrating axisymmetric surface also emanates acoustic waves. A shape optimizing process may be applied to the transducer to generate an acoustically more effective concentrator. The shape changes in the BE mesh are much smaller than the FEM counterpart, leading to a faster shape optimization process.

In this article, Frequency Response Functions (FRF) of axisymmetric bodies with known analytical eigenfrequencies and eigenmodes are used to validate the implementation. Furthermore the eigenfrequencies of a typical acoustic concentrator with arbitrary axisymmetric geometry are obtained by the peaks of the system FRF. At these peaks operational modes are recovered and displayed.

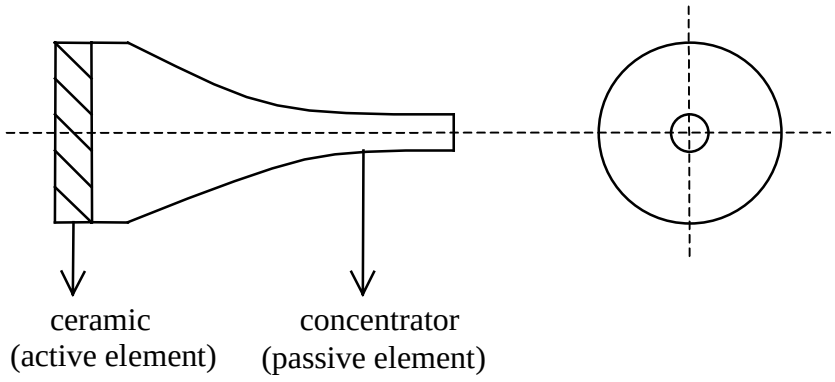

Figure 1 – Ultrasonic transducer

2. GOVERNING DIFFERENTIAL EQUATIONS

The dynamic behavior of the linear, elastic homogeneous and isotropic body is governed by Navier's equations [Graff, 1975; Dominguez, 1993]. In terms of the continuum displacements components u_i these equations are:

$$\mu\, u_{i,jj} + (\lambda + \mu)\, u_{j,ji} + b_i = \rho\, \ddot{u}_i \qquad (1)$$

In eqn (1) b_i is the *i-th* component of the body force vector, λ and μ are Lame's constants and ρ is the continuum density. The dots over the displacement component means derivation with respect to time. Considering the stationary case, $u(x,t) = u(x)\,exp(i\omega t)$ with circular frequency ω, eqn (1) may be written as:

$$\mu\, u_{i,jj} + (\lambda + \mu)\, u_{j,ji} + b_i = -\omega^2 \rho\, u_i \qquad (2)$$

Introducing the continuum dilatation and shear wave velocities, respectively, $C_p^2=(\lambda\ +2\mu\ )/\rho$ and $C_s^2=\mu\ /\rho$, eqn (2) may be recast into [Graff, 1975; Dominguez, 1993]:

$$Cs^2 u_{i,jj} + \left(Cp^2 - Cs^2\right) u_{j,ji} + b_i = -\omega^2 u_i \qquad (3)$$

The solution of eqn (3) for axisymmetric bodies subjected to prescribed boundary conditions is the aim of the present article. The equation governing the corresponding static problem is obtained setting the inertial forces equal to zero, *($\rho\ \ \omega^{\ 2} u_i$ = 0)*.

3. BOUNDARY INTEGRAL EQUATIONS - BIE

3.1. The 3D equations

Using Betti's reciprocity theorem or a standard Weighted Residual procedure the differential eqn (3) can be transformed into an integral equation over the boundary *S* of the 3D domain. Neglecting the body forces *(b_i=0)*, the 3D equations can be written as [Dominguez, 1993]:

$$c_{ij} u_j(\xi) = \int_S u_{ij}^*(\xi, x) t_i(x)\, dS(x) - \int_S t_{ij}^*(\xi, x) u_i(x)\, dS(x) \qquad (4)$$

In eqn (4) the displacements and tractions of problem being solved are represented by u_i and t_i, respectively. The collocation point is ξ and the field point is *x*. The elements of c_{ij} are called integration free terms. Equation (4) describes both the elastostatic and the elastodynamic problem, according to the fundamental solution employed. If the kernels of the static fundamental solution $u_{ij}^*=u^*_{ijSTA}$, $t_{ij}^*=t^*_{ijSTA}$ are applied, eqn (4) describes the static problem [Becker, 1992]. If the stationary dynamic kernels $u_{ij}^*=u^*_{ijDYN}$, $t_{ij}^*=t^*_{ijDYN}$ are considered, the equation describes the stationary dynamic problem [Dominguez, 1993]. It is important to mention that the static and dynamic 3D displacement and traction kernels present singularities of the order *O(1/r)* and *O($1/r^2$)*, respectively.

3.2. The axisymmetric equations

To synthesize the Axisymmetric BIE from eqn (4), a coordinate transformation from the cartesian system (3D) to a cylindrical system (AXI) is performed. Figure 2 shows the axial *z*, radial *r* and azimuthal θ directions of the cylindrical coordinate system.

The surface integration over the 3D boundary *S* in eqn (4) is divided into an integration over the azimuthal direction θ and an integration over the line generation the revolution surface Γ. The integration over θ will render the axisymmetric kernels u^*_{ijAXI}, t^*_{ijAXI} that must be integrated over Γ [Emperador, Dominguez, 1989; Wang, Banerjee, 1990].

$$\int_S u_{ij}^*(\xi, x)\, dS(x) = \int_\Gamma \left[\int_\theta u_{ij}^*(r, z, \theta)\, d\theta\right] d\Gamma(r, z) = \int_\Gamma u^*_{ijAXI}(r, z)\, d\Gamma(r, z) \qquad (5)$$

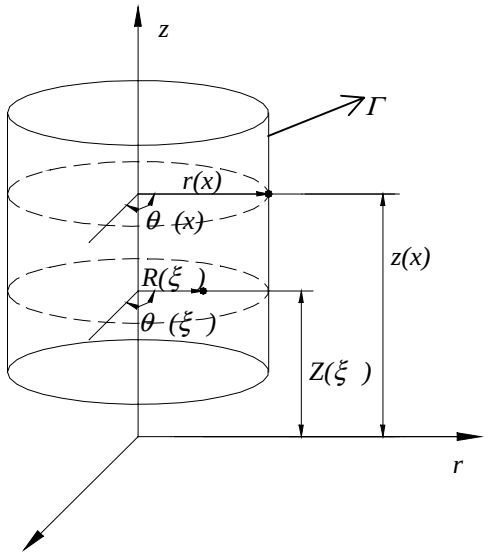

Figure 2: Definitions for the cylindrical coordinate system

After the integration is performed the equations in the *rz* plane are uncoupled from the θ direction, resulting in a 2D system of integral equations [Becker, 1992]:

$$\begin{bmatrix} c_{11} & c_{12} \\ c_{21} & c_{22} \end{bmatrix} \begin{bmatrix} u_r(\xi) \\ u_z(\xi) \end{bmatrix} + 2\pi \int_\Gamma \begin{bmatrix} t^*_{rr}(\xi,x) & t^*_{rz}(\xi,x) \\ t^*_{zr}(\xi,x) & t^*_{zz}(\xi,x) \end{bmatrix} \begin{bmatrix} u_r(x) \\ u_z(x) \end{bmatrix} r(x)\, d\Gamma(x) = 2\pi \int_\Gamma \begin{bmatrix} u^*_{rr}(\xi,x) & u^*_{rz}(\xi,x) \\ u^*_{zr}(\xi,x) & u^*_{zz}(\xi,x) \end{bmatrix} \begin{bmatrix} t_r(x) \\ t_z(x) \end{bmatrix} r(x)\, d\Gamma(x) \tag{6}$$

In eqn (6) the collocation point ξ and the field point *x* have, respectively, the coordinates $(R(\xi), \theta(\xi), Z(\xi))$ and $(r(x), \theta(x), z(x))$. This integral equation is also valid for the static and for the stationary dynamic case. The integral equation (6) can now be discretized as in the standard Boundary Element procedure. The only difficulties to be overcome are the element integrations over the weak and strong singular kernels.

3.3. Integration over singular elements

Static case, weak singularities. The displacement kernels $u_{ij}(i, j = r, z)$ in eqn (6) present weak singularities. These kernels can be rearranged, so that the (weak) singular integrals are represented as elliptical integrals of the first and second kind, *K(m,π /2)* and *E(m,π /2)*, which can be evaluated by Gaussian quadrature [Becker, 1992; Carrion, 1999]. In full extend, the static axisymmetric kernels are:

$$u_{rr}(\xi,x)=\frac{A}{R(\xi)\,r(x)\,C}\left\{\begin{array}{l}\left[3-4\nu+\left[R(\xi)^2+r(x)^2+(Z(\xi)-z(x))^2\right]+(Z(\xi)-z(x))^2\right]\\ K\left(m,\pi/2\right)+\\ \left[-C^2(3-4\nu)-\dfrac{(Z(\xi)-z(x))^2\left[R(\xi)^2+r(x)^2+(Z(\xi)-z(x))^2\right]}{D}\right]\\ E\left(m,\pi/2\right)\end{array}\right\} \tag{7a}$$

$$u_{rz}(\xi,x)=\frac{A\,(Z(\xi)-z(x))}{R(\xi)\,C}\left\{K\left(m,\pi/2\right)-\frac{r(x)^2-R(\xi)^2+(Z(\xi)-z(x))^2}{D}E\left(m,\pi/2\right)\right\} \tag{7b}$$

$$u_{zr}(\xi,x)=\frac{A\,(Z(\xi)-z(x))}{r(x)\,C}\left\{-K\left(m,\pi/2\right)+\frac{R(\xi)^2-r(x)^2+(Z(\xi)-z(x))^2}{D}E\left(m,\pi/2\right)\right\} \tag{7c}$$

$$u_{zz}(\xi,x)=\frac{2A}{C}\left\{(3-4\nu)K\left(m,\pi/2\right)+\frac{(Z(\xi)-z(x))^2}{D}E\left(m,\pi/2\right)\right\} \tag{7d}$$

where:

$$A=\frac{1}{16\pi^2\mu\,(1-\nu)} \tag{8a}$$

$$C=\left[(R(\xi)+r(x))^2+(Z(\xi)-z(x))^2\right]^{1/2} \tag{8b}$$

$$D=(R(\xi)-r(x))^2+(Z(\xi)-z(x))^2 \tag{8c}$$

Static case, strong singularities. The strong singular static traction kernels in equation (6) are integrated using the rigid body argument for the axial *z* direction and the solution of a particular state of stress for the radial *r* direction [Becker, 1992; Carrion, 1999].

Dynamic case, weak and strong singularities. It is not possible to apply the rigid body argument to the strong singular dynamic traction kernels. But the dynamic kernels present the same order of singularity of the static kernels [Dominguez, 1993]. So it is possible to regularize the strong integrals, subtracting the static kernels from the dynamic ones. This strategy will be applied to the weak and strong singular dynamic kernels, as described below. Assuming the following convention for the indexes:

3D = tridimensional problem in cartesian coordinates
AXI = axisymmetric problem in cylindrical coordinates
STA = static problem
DYN = dynamic problem

Equation (4) can be written for the dynamic (ω) case as:

$$c_{ij}\ u_j(\xi,\omega) = \int_S \left\{ u^*_{ij(3D,DYN)}\ t_i - t^*_{ij(3D,DYN)}\ u_i \right\} dS(x) \tag{9}$$

Subtracting and adding the 3D static kernels from eqn (9) results:

$$c_{ij}u_j(\xi,\omega) = \int_S u^*_{ij(3D,DYN)}\ t_i\ dS(x) - \int_S u^*_{ij(3D,STA)}\ t_i\ dS(x) + \int_S u^*_{ij(3D,STA)}\ t_i\ dS(x) -$$

$$\int_S t^*_{ij(3D,DYN)}\ u_i\ dS(x) - \int_S t^*_{ij(3D,STA)}\ u_i\ dS(x) + \int_S t^*_{ij(3D,STA)}\ u_i\ dS(x) \tag{10}$$

If equation (10) is transformed into an axisymmetric problem, it may be written as:

$$c_{ij}u_j(\xi,\omega) = \int_\Gamma \int_0^{2\pi} \left[u^*_{ij(3D,DYN)} - u^*_{ij(3D,STA)} \right] t_i\ d\theta\ d\Gamma(x) + \int_\Gamma \int_0^{2\pi} u^*_{ij(3D,STA)}\ t_i\ d\theta\ d\Gamma(x) -$$

$$\int_\Gamma \int_0^{2\pi} \left[t^*_{ij(3D,DYN)} - t^*_{ij(3D,STA)} \right] u_i\ d\theta\ d\Gamma(x) + \int_\Gamma \int_0^{2\pi} t^*_{ij(3D,STA)}\ u_i\ d\theta\ d\Gamma(x) \tag{11}$$

or still:

$$c_{ij}u_j(\xi,\omega) = \int_\Gamma \int_0^{2\pi} \left[u^*_{ij(3D,DYN)} - u^*_{ij(3D,STA)} \right] t_i\ d\theta\ d\Gamma(x) + \int_\Gamma u^*_{ij(AXI,STA)}\ t_i\ d\Gamma(x) -$$

$$\int_\Gamma \int_0^{2\pi} \left[t^*_{ij(3D,DYN)} - t^*_{ij(3D,STA)} \right] u_i\ d\theta\ d\Gamma(x) + \int_\Gamma t^*_{ij(AXI,STA)}\ u_i\ d\Gamma(x) \tag{12}$$

The integrals in eqn (12) containing the difference of the dynamic and static kernels are no longer singular and may be evaluated by standard quadrature methods. The values of the integrals over the singular static kernels are obtained by the rigid body procedure mentioned in the previous section.

4. NUMERICAL EXAMPLES

4.1. Validation – static problem

Since the solution of the dynamic problem makes use of the static solution to regularize the singular integrals, the static implementation will be validated. The example is a cylinder fixed at one end and loaded uniformly at the other free extremity. The ratio of the diameter to the length is 1/10 (see Figure 3). This axisymmetric problem was solved with constant elements. All integrations were performed with 4 Gauss points. Table 1, shows the normalized displacement obtained at the point (r = 0.05, z = 10.0) for three distinct discretizations. An analytical solution is also presented. The solution is very good for the 32 elements case, indicating that the static implementation could be considered correct.

Table 1: Normalized static displacement for the cylinder

ANALYTICAL	BEM-AXI (8 elements)	BEM-AXI (16 elements)	BEM-AXI (32 elements)
1.00	0.53	0.95	1.00
Relative error	47%	5%	0%

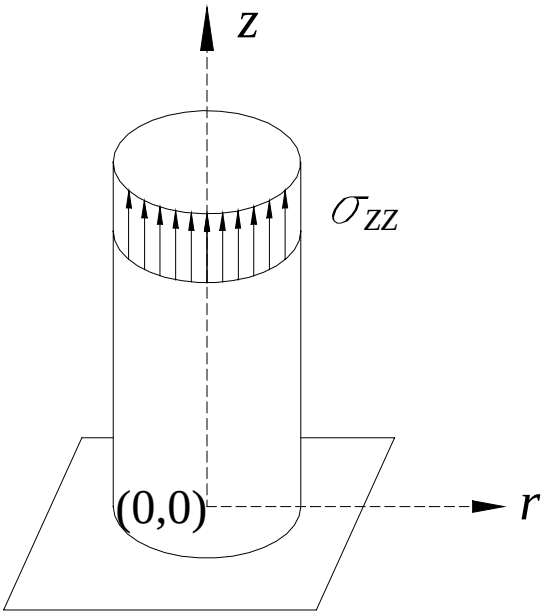

Figure 3: A free-fixed cylinder subjected to a uniform loading.

4.2. Validation – dynamic problem

To validate the dynamic implementation, the Frequency Response Function (FRF) of the cylinder shown in Figure 3 is determined. Figure 4a shows the normalized FRF measured at the same point where the static displacement was determined. The used mesh has 32 axisymmetric elements. The frequencies were normalized with respect to the first eigenfrequency of the analytical solution. The FRF was obtained for 256 frequency points. The eigenfrequencies for the BEM-AXI implementation were obtained from the local maxima of the FRF. Table 2 shows the values of the normalized eigenfrequencies obtained from the FRF peaks and compared to the analytical solution. At the frequencies corresponding to the FRF peaks the operational modes were determined. Figures 4b, 4c and 4d show the first three operational modes of the cylinder obtained from the BEM-AXI implementation, compared to the analytical solution. It can be seen that there is a very good agreement between numerical and analytical solutions, leading to the conclusion that the present dynamic axisymmetric formulation and implementation is correct.

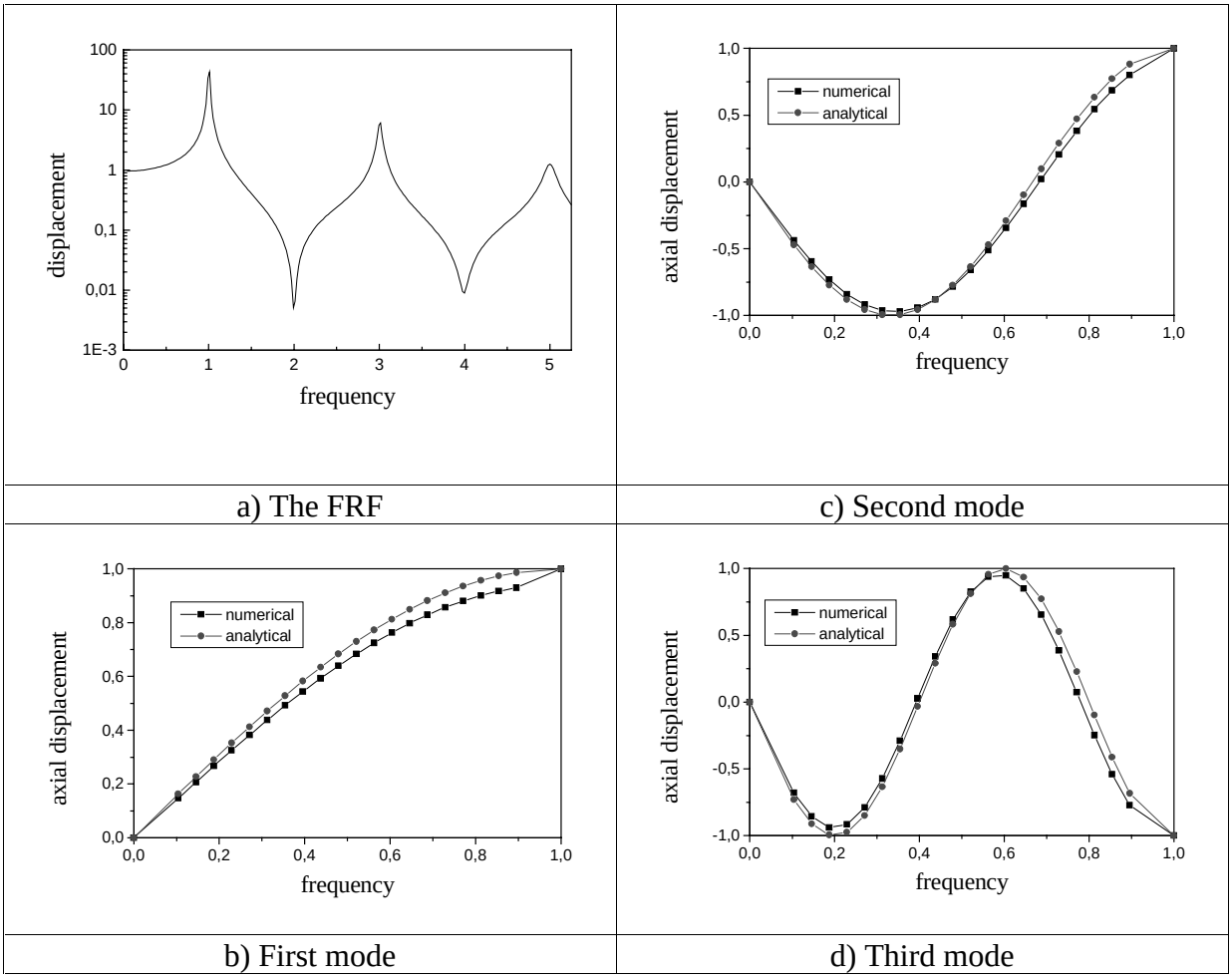

Figure 4: Dynamic response of the cylinder

Table 2: Normalized eigenfrequencies for the cylinder

Freq. N.	ω_1	ω_3	ω_5
Analytical	1.00	3.00	5.00
BEM-AXI 16 elements	0.99	2.99	5.00
Relative error	1%	1%	0%
BEM-AXI 32 elements	0.99	2.99	5.00
Relative error	1%	1%	0%
BEM-AXI 64 elements	0.99	2.99	5.00
Relative error	1%	1%	0%

4.3. Dynamic response of an acoustic horn

The methodology developed and validated in the previous sections is applied to a typical acoustic horn, used in ultrasonic transducers [Eisner, 1967]. Figure 6 shows the investigated horn. It is an axisymmetric body with a cross sectional area varying according to the law $d(z)=d(0)[1-(z/L)^{0.5}]+d(L)(z/L)^{0.5}$. The horn is considered as a free-free element. The excitation is applied at the bottom and the displacement is determined at the top.

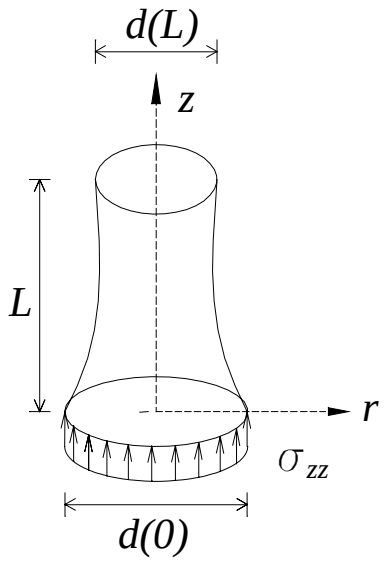

Figure 5: Definitions for the acoustic horn.

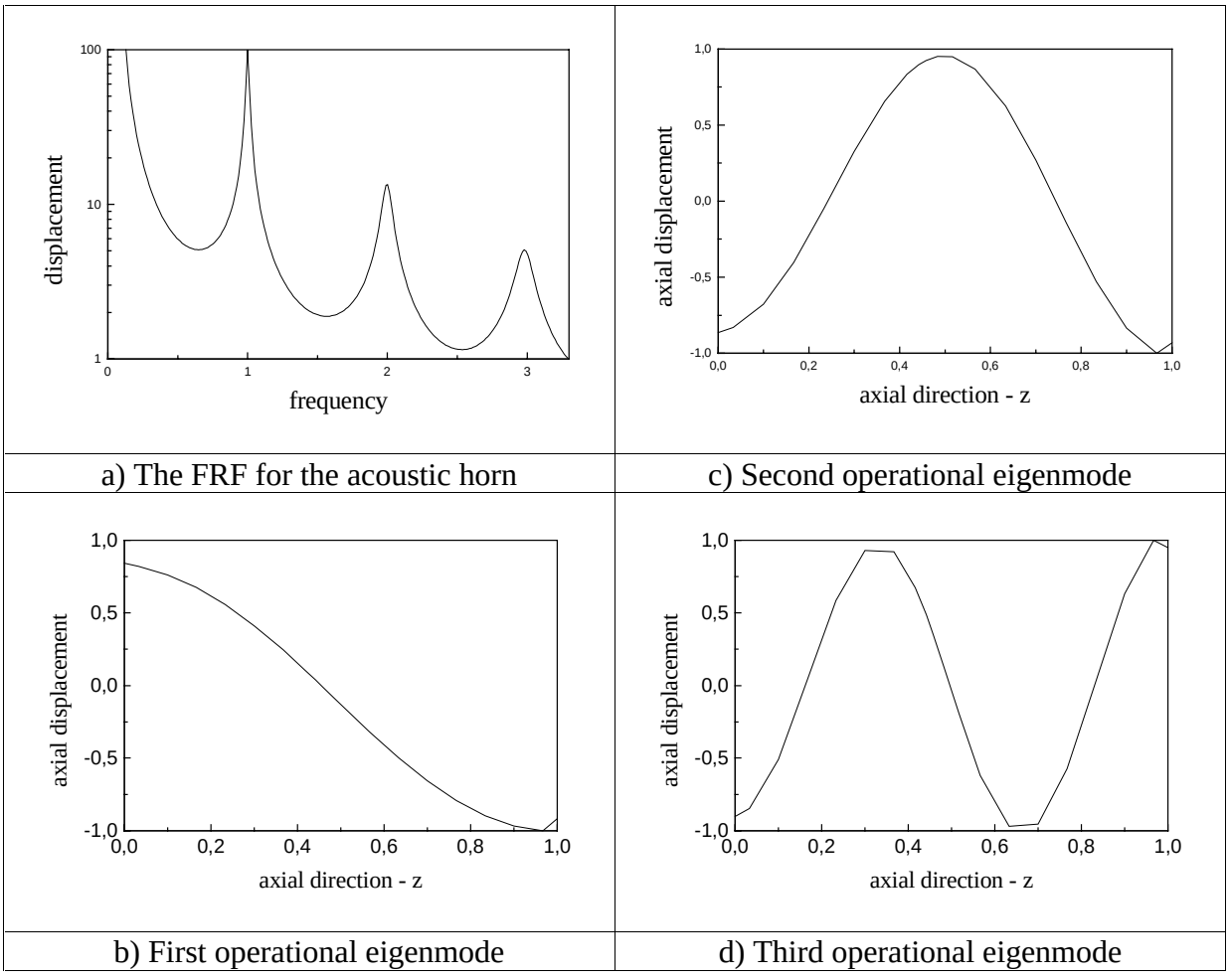

a) The FRF for the acoustic horn

c) Second operational eigenmode

b) First operational eigenmode

d) Third operational eigenmode

Figure 6: The first 3 operational eigenmodes of the acoustic horn.

The FRF obtained for the free-free horn is given in Figure 6. It can be seen that at low frequencies the displacement is very large, corresponding to the rigid body translation. Figure 6a show three peaks in the FRF corresponding to 3 eigenfrequencies. The operational eigenmodes associated to the 3 FRF peaks can be seen in Figures 6b, 6c e 6d.

The transducer operational eigenmodes can be used to determine the position of the nodes where the transducer may be fixed. Fixing the transducer at the node of one eigenmode should uncouple the transducer dynamic response from the dynamic behavior of the fixing support.

5. CONCLUDING REMARKS

In the present article a numerical tool to analyze the dynamic response of axisymmetric elastic bodies based on the Boundary Element Methodology is presented. The axisymmetric formulation is discussed in some extent. The procedures to integrate weak and strong singular elements are outlined. The methodology was validated by means of comparisons with analytical solutions. The method is used, exemplarily, to obtain modal data, eigenfrequencies and eigenmodes of an acoustic horn.

6. REFERENCES

Becker, A. A., 1992, The Boundary Element Method in Engineering - A complete course, McGraw-Hill Book Company.

Carrion, R., 1999, Boundary Element Method in Axysimmetric Elastodynamic, MSc. Dissertation (in Portuguese), Biomedical Engineering Dept., State University of Campinas – UNICAMP,

Dominguez, J., 1993, Boundary Elements in Dynamics, Computacional Mechanics Publications.

Eisner, E., 1967, Complete Solutions of the “Webster” Horn Equation, The Journal of Acoustical Society of America, vol. 41, n. 4, part 2, pp. 1126-1146.

Emperador, J. M., Dominguez, J., 1989, Dynamic Response of Axisymmetric Embedded Foundations, Earthquake Engineering and Structural Dynamics, vol.18, pp. 1105-1117.

Graff, K. F., 1975, Wave Motion in Elastic Solids, Dover Publications.

Kane, J. H., 1994, Boundary Element Analysis in Engineering Continuum Mechanics, Prentice Hall.

Wang, H. C., Banerjee, P. K., 1990, Generalized Axisymmetric Elastodynamic Analysis by Boundary Element Method, International Journal for Numerical Methods in Engineering, vol. 30, pp. 115-131.